REFERENCES AND NOTES

1. G. Odian, *Principles of Polymerization* (Wiley, New York, ed. 3, 1981), chaps. 3 and 4.
2. R. Arshady, *Colloid Polym. Sci.* **270**, 717 (1992).
3. K. E. J. Barrett, *Dispersion Polymerization in Organic Media* (Wiley, London, 1975).
4. S. Shen, E. D. Sudol, M. S. El-Aasser, *J. Polym. Sci. Part A* **32**, 1087 (1994).
5. D. H. Napper, *Polymeric Stabilization of Colloidal Dispersions* (Academic Press, London, 1983).
6. E. Matijevic, *Surface and Colloid Science* (Plenum, New York, 1993), vol. 15.
7. R. M. Fitch, *Polymer Colloids* (Plenum, New York, 1971).
8. J. M. DeSimone, Z. Guan, C. S. Elsbernd, *Science* **257**, 945 (1992).
9. Z. Guan, J. R. Combes, Y. Z. Menceloglu, J. M. DeSimone, *Macromolecules* **26**, 2663 (1993).
10. J. R. Combes, Z. Guan, J. M. DeSimone, *ibid.* **27**, 865 (1994).
11. Z. Guan, C. S. Elsbernd, J. M. DeSimone, *Polym. Prepr. Am. Chem. Soc. Div. Polym. Chem.* **33**, 329 (1992).
12. Z. Guan, J. R. Combes, C. S. Elsbernd, J. M. DeSimone, *ibid.* **34**, 447 (1993).
13. T. Hoefling, D. Stofesky, M. Reid, E. J. Beckman, R. M. Enick, *J. Supercrit. Fluids* **5**, 237 (1992).
14. T. A. Hoefling, D. A. Newman, R. M. Enick, E. J. Beckman, *ibid.* **6**, 165 (1993).
15. K. A. Consani and R. D. Smith, *ibid.* **3**, 51 (1990).
16. R. M. Lemert, R. A. Fuller, K. P. Johnston, *J. Phys. Chem.* **94**, 6021 (1990).
17. D. G. Peck and K. P. Johnston, *ibid.* **95**, 9549 (1991).
18. G. J. McFann and K. P. Johnston, *ibid.*, p. 4889.
19. J. M. DeSimone, E. E. Maury, J. R. Combes, Y. Z. Menceloglu, *Polym. Prepr. Am. Chem. Soc. Div. Polym. Mater. Sci. Eng.* **68**, 41 (1993).
20. We have also reported on the synthesis and solubility characteristics of graft copolymers that have a fluorocarbon backbone [based on poly(1,1-dihydroperfluorooctyl acrylate)] either with hydrophilic grafts [based on poly(ethylene oxide)] or with hydrocarbon grafts (based on polystyrene) that have the appropriate solubility characteristics to also be effective surfactants for CO_2; see E. E. Maury *et al.*, *Polym. Prepr. Am. Chem. Soc. Div. Polym. Chem.* **34**, 664 (1993). We have also designed high molar mass triblock copolymers that contain fluorocarbon and hydrocarbon segments for utilization as surfactants and viscosity modifiers for CO_2; see Z. Guan and J. M. DeSimone, *ibid.*, p. 614.
21. P. D. Condo, D. R. Paul, K. P. Johnston, *Macromolecules* **27**, 365 (1994).
22. Percent conversions were determined gravimetrically. We determined molar masses by gel permeation chromatography (GPC) on a Waters 150-CV gel permeation chromatograph with Ultrastyragel columns of 100, 500, 10^3, and 10^4 Å porosities, using a tetrahydrofuran mobile phase and polystyrene standards (Showa Denko). We measured the average particle size by SEM.
23. Molar masses were determined at 3M by GPC on a Waters 410 DRI with a Jordi Associates Mixed Bed column packed in Freon-113 with a Freon-113 mobile phase.
24. I. Piirma, *Polymeric Surfactants* (Dekker, New York, 1992).
25. M. McHugh and V. Krukonis, *Supercritical Fluid Extraction* (Butterworth-Heinemann, Boston, ed. 2, 1994).
26. C. M. Tseng, Y. Y. Lu, M. S. El-Asser, J. W. Vanderhoff, *J. Polym. Sci. Polym. Chem. Ed.* **24**, 2995 (1986).
27. Y. Y. Lu, M. S. El-Asser, J. W. Vanderhoff, *J. Polym. Sci. Polym. Phys. Ed.* **26**, 1187 (1988).
28. Union Carbide Chemicals & Plastics has developed a coating technology that replaces up to 80% of the solvents normally used in spray-coating formulations with CO_2. We believe that with the use of surfactants, coating processes could be developed with 100% of the solvents replaced by CO_2 for certain applications (perhaps in conjunction with a coalescing agent).

29. We are grateful to the National Science Foundation for a Presidential Faculty Fellowship (J.M.D.: 1993 through 1997) as well as to DuPont, 3M, and Unilever for financial support. In addition, we thank Isco Corporation for the use of their syringe pump, R. Spontak and D. Batchelor for assistance with the electron microscopy, and C. Elsbernd for GPC analysis using a Freon-113 mobile phase.

29 March 1994; accepted 18 May 1994

Catalytic Activation of Carbon–Fluorine Bonds by a Soluble Transition Metal Complex

Michael Aizenberg and David Milstein*

Homogeneous catalytic activation of the strong carbon–fluorine bonds under mild conditions was achieved with the use of rhodium complexes as catalysts. The catalytic reactions between polyfluorobenzenes and hydrosilanes result in substitution of fluorine atoms by hydrogen atoms and are chemo- and regioselective. With individual stoichiometric steps observed and combined, and with intermediates isolated and fully characterized (including crystal structures), these systems demonstrate the effectiveness of a rational approach to catalytic design.

Homogeneous catalysis by transition metal complexes has an important role in chemistry, enabling efficient, selective processes under mild, easily controllable conditions and leading to the production of millions of tons of chemicals annually (*1*). These processes are based on the activation of chemical bonds by transition metals, followed by transformations in the metal coordination sphere and product release. Despite the phenomenal growth of this field, homogeneous catalysis by a metal complex based on activation of the strongest bond that carbon can form, C–F, remains unknown. Such catalysis is highly desirable for the functionalization of polyfluorinated organic compounds, which are important constituents of the chemical, pharmaceutical, and advanced materials industries (*2*). Toward this goal, much research effort has been devoted to the activation of the strong C–F bond by transition metal complexes. Indeed, C–F bond cleavage, although still fairly uncommon, is now known in a number of intermolecular systems involving transition metal complexes (*3–5*). However, despite this remarkable progress, all of these reactions are stoichiometric. We report here that aromatic C–F bonds can be cleaved by rhodium complexes even at room temperature and that this reaction can be elaborated into homogeneous catalysis involving C–F bonds. These catalytic cycles, which were designed by a combination of individual stoichiometric reactions, exhibit high selectivity.

The Rh(I) silyl complex $L_3RhSiMe_2Ph$ (**1a**) ($L = PMe_3$), synthesized from L_4RhCl and $LiSiMe_2Ph$ and structurally characterized (*6, 7*), reacts quantitatively with C_6F_6 at room temperature:

$$\underset{\substack{\textbf{1a},\ R_3 = Me_2Ph \\ \textbf{1b},\ R_3 = Ph_3}}{L_3RhSiR_3} + C_6F_6 \rightarrow \underset{\textbf{2}}{L_3RhC_6F_5} + R_3SiF \qquad (1)$$

The Me_2PhSiF product was identified unambiguously by ^{19}F and ^1H nuclear magnetic resonance (NMR) and by gas chromatography–mass spectroscopy (*8*). Complex **2** was characterized spectroscopically (*7*), and its identity was confirmed by an x-ray crystallographic study (*7*) (Fig. 1) and by its independent synthesis from L_4RhCl and C_6F_5MgBr. Interestingly, the

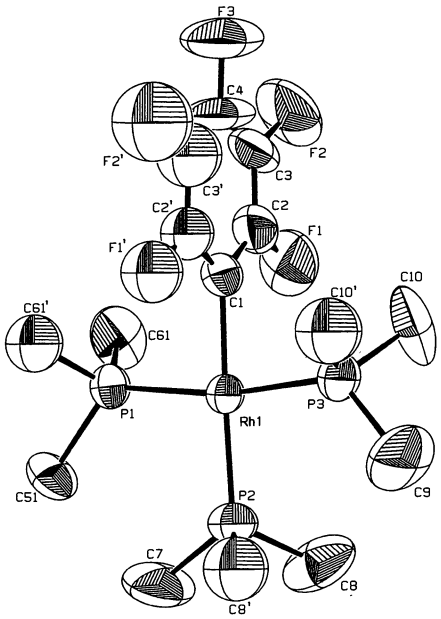

Fig. 1. Perspective view (ORTEP) of **2** (hydrogen atoms are omitted for clarity). Bond distances and angles (errors in last digits in parentheses) are Rh1-P1 = 2.292(2) Å; Rh1-P2 = 2.258(3) Å; Rh1-P3 = 2.291(2) Å; Rh1-C1 = 2.078(8) Å; P1-Rh1-P3 = 169.4(1)°; and P2-Rh1-C1 = 177.8(2)°.

Department of Organic Chemistry, Weizmann Institute of Science, Rehovot 76100, Israel.

*To whom correspondence should be addressed.

distance between Rh and P2 is shorter than that between Rh and P1, indicating a weak C_6F_5 trans effect. The complex $L_3RhSiPh_3$ (9), **1b**, reacts similarly, but heating at 90°C is required.

Pentafluorobenzene (C_6F_5H) is also reactive, although less so than C_6F_6. When **1a** is heated with excess C_6F_5H to 110°C in a closed vessel, quantitative C–F activation takes place to produce Me_2PhSi–F and tetrafluorobenzene ($C_6F_4H_2$). Interestingly, the organometallic product is, again, **2**. A likely mechanism involving consecutive C–F and C–H activation accounts for these results (reactions 2 and 3). The overall stoichiometry is shown in reaction 4:

$$L_3RhSiMe_2Ph + C_6F_5H \xrightarrow[\text{activation}]{\text{C–F}} L_3Rh(C_6F_4H) + FSiMe_2Ph \quad (2)$$

$$L_3Rh(C_6F_4H) + C_6F_5H \xrightarrow[\text{activation}]{\text{C–H}} L_3RhC_6F_5 + C_6F_4H_2 \quad (3)$$

$$L_3RhSiMe_2Ph + 2C_6F_5H \rightarrow L_3RhC_6F_5 + C_6F_4H_2 + FSiMe_2Ph \quad (4)$$

Activation of the weaker C–H bond is generally preferred to C–F cleavage (*4, 10*), although competition between the two has been demonstrated in intramolecular systems (*11*). Here, the direction of the reaction is thermodynamically driven by the irreversible formation of the very strong Si–F bond (*12*).

Complex **2** reacts with 1 equivalent of Ph_3SiH at 90°C to yield **1b** and C_6F_5H, as observed by ^{31}P, ^{1}H, and ^{19}F NMR:

$$L_3RhC_6F_5 + Ph_3SiH \rightarrow C_6F_5H + L_3RhSiPh_3 \quad (5)$$

Although an oxidative addition intermediate was not observed in this case, its analog **3** can be easily isolated from the reaction of **2** with $(EtO)_3SiH$ at room temperature:

$$L_3RhC_6F_5 + (EtO)_3SiH \longrightarrow$$

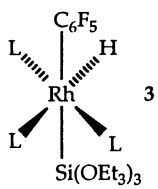

3 (6)

The meridional configuration with H trans to PMe_3 and cis to both C_6F_5 and $(EtO)_3Si$ ligands unequivocally follows from ^{31}P, ^{1}H, and ^{19}F NMR data (*7*) and is confirmed by an x-ray crystallographic study (Fig. 2) (*7*). The weak trans effect of C_6F_5 is manifested here as well, locating the strong trans director, R_3Si, opposite C_6F_5.

The heating of **3** at 95°C yields C_6F_5H. We have recently shown that C–Si and C–H bond formation can proceed at competitive rates (*13*). In this case, only C–H formation takes place, undoubtedly because of the trans C_6F_5 and SiR_3 arrangement. This results in regeneration of the Rh–Si complex and, together with the other reactions presented here, provides a basis for the design of a novel catalytic cycle (Fig. 3). Indeed, reaction of complex **2** with excess C_6F_6 and R_3SiH (R = Ph or EtO) at 90°C leads to catalytic F substitution by H, yielding C_6F_5H and R_3SiF. The $(EtO)_3SiH$ reacts more efficiently than Ph_3SiH, probably because of easier oxidative addition of the former. This reaction is selective; C_6F_5H is less reactive than C_6F_6. This reactivity goes against the expected trend in hydrogenolysis of polyhaloaromatic compounds (*14*).

Highly regioselective catalysis was observed upon reaction of C_6F_5H with $(EtO)_3SiH$ and **2**, which leads exclusively to 1,4-$C_6F_4H_2$:

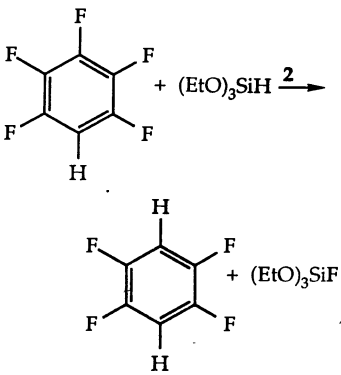

(7)

The mechanism of this reaction is analogous to the one outlined in Fig. 3 (*15*).

Products resulting from C–Si coupling were not observed in any of these cases, again because of the stereochemistry of the intermediate **3**. Although we did not optimize the catalytic reactions, several tens of turnovers were achieved (*16*).

Some mechanistic considerations regarding the C–F activation step are appropriate here. We observed that **1a** reacts most easily with C_6F_6, whereas the reaction with C_6F_5H is more difficult and C_6H_5F does not undergo C–F bond cleavage under reaction conditions. This reactivity trend parallels the order of electron affinities of these fluorocarbons (*17*). On the other hand, C–F bond dissociation energies in these compounds follow the opposite trend, with the C_6H_5–F bond ~30 kcal mol^{-1} weaker than the C_6F_5–F bond (*18*). On this basis, we favor as an explanation the electron transfer from the complex to the substrate and generation of $C_6F_6^{\cdot -}$ (*5*), followed by F^- attack on silicon. A mechanism involving metal insertion into C–F (oxidative addition), followed by Si–F elimination may also be possible (*19*). It should be noted, however, that oxidative addition reactions of partially fluorinated arenes with Rh(I) (and other metals) resulted in C–H rather than C–F activation (*10*).

We have shown that Rh(I) silyls easily cleave C–F bonds of C_6F_6 and C_6F_5H, even (in the latter case) in preference to the C_6F_5–H bond. These reactions, combined with Si–H oxidative addition and C–H reductive elimination, present examples of catalytic cycles involving C–F activation by a metal complex. Moreover, we have observed catalytic chemo- and regioselectivity (*20*).

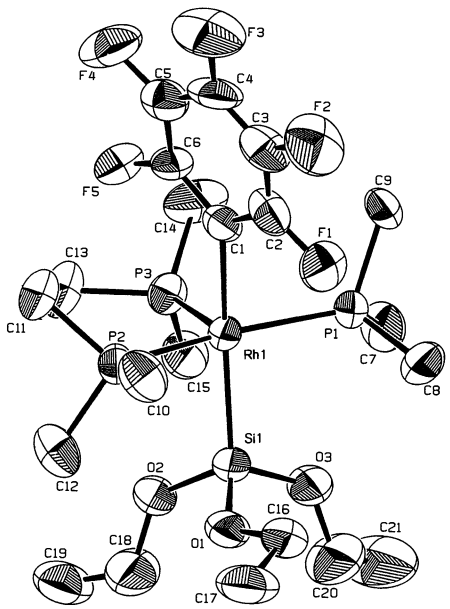

Fig. 2. Perspective view (ORTEP) of **3** (hydrogen atoms are omitted for clarity) (*21*). Bond distances and angles (errors in last digits in parentheses) are Rh1-P1 = 2.307(4) Å; Rh1-P2 = 2.316(4) Å; Rh1-P3 = 2.388(5) Å; Rh1-Si1 = 2.325(4) Å; Rh1-C1 = 2.24(1) Å; P1-Rh1-P2 = 163.1(2)°; and Si1-Rh1-C1 = 163.0(4)°.

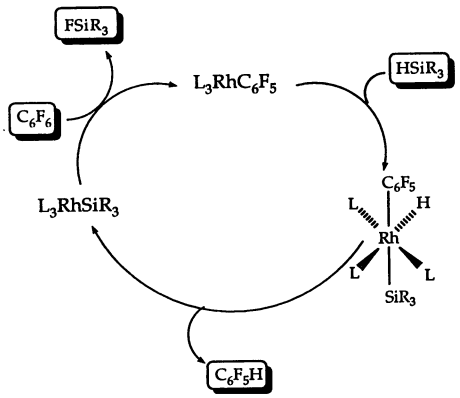

Fig. 3. Catalytic cycle for F and H exchange between hexafluorobenzene and hydrosilanes.

REFERENCES AND NOTES

1. G. W. Parshall and S. D. Ittel, *Homogeneous Catalysis* (Wiley, New York, ed. 2, 1992).
2. M. Grayson, Ed., *Kirk-Othmer Concise Encyclopedia of Chemical Technology* (Wiley, New York, 1985), pp. 505–518.
3. D. R. Fahey and J. E. Mahan, *J. Am. Chem. Soc.* **99**, 2501 (1977); M. T. Jones and R. N. McDonald, *Organometallics* **7**, 1221 (1988); C. J. Burns and R. A. Andersen, *J. Chem. Soc. Chem. Commun.* **1989**, 136 (1989); P. L. Watson, T. H. Tulip, I. Williams, *Organometallics* **9**, 1999 (1990); W. D. Jones, M. G. Partridge, R. N. Perutz, *J. Chem. Soc. Chem. Commun.* **1991**, 264 (1991); P. Hofmann and G. Unfried, *Chem. Ber.* **125**, 659 (1992); S. Hintermann, P. S. Pregosin, H. Rüegger, H. C. Clark, *J. Organomet. Chem.* **435**, 225 (1992); A. H. Klahn, M. H. Moore, R. N. Perutz, *J. Chem. Soc. Chem. Commun.* **1992**, 1699 (1992); R. G. Harrison and T. G. Richmond, *J. Am. Chem. Soc.* **115**, 5303 (1993); M. Weydert, R. A. Andersen, R. G. Bergman, *ibid.*, p. 8837.
4. S. T. Belt, M. Helliwell, W. D. Jones, M. G. Partridge, R. N. Perutz, *J. Am. Chem. Soc.* **115**, 1429 (1993).
5. O. Blum, F. Frolow, D. Milstein, *J. Chem. Soc. Chem. Commun.* **1991**, 258 (1991).
6. M. Aizenberg and D. Milstein, unpublished results. The x-ray structure of **1a** is not shown here. Abbreviations: Ph, phenyl; Me, methyl; Et, ethyl.
7. Supplementary material is available from the authors, including experimental procedures and characterization for complexes **1a**, **2**, and **3** and full x-ray structural data of complexes **2** and **3**.
8. For the mass spectrometry of Me_2PhSiF, see G. Dube and E. Gey, *Org. Mass Spectrom.* **14**, 17 (1979).
9. Prepared according to D. L. Thorn and R. L. Harlow, *Inorg. Chem.* **29**, 2017 (1990).
10. M. I. Bruce, B. L. Goodall, G. L. Sheppard, F. G. A. Stone, *J. Chem. Soc. Dalton Trans.* **1975**, 591 (1975); C. M. Anderson, R. J. Puddephatt, G. Ferguson, A. J. Lough, *J. Chem. Soc. Chem. Commun.* **1989**, 1297 (1989); A. D. Selmeczy, W. D. Jones, M. G. Partridge, R. N. Perutz, *Organometallics* **13**, 522 (1994).
11. M. Crespo, M. Martinez, J. J. Sales, *J. Chem. Soc. Chem. Commun.* **1992**, 822 (1992); *Organometallics* **12**, 4297 (1993); B. L. Lucht, M. J. Poss, M. A. King, T. G. Richmond, *J. Chem. Soc. Chem. Commun.* **1991**, 400 (1991).
12. R. Walsh, in *The Chemistry of Organic Silicon Compounds*, S. Patai and Z. Rappoport, Eds. (Wiley, New York, 1989), vol. 1, chap. 5.
13. M. Aizenberg and D. Milstein, *Angew. Chem. Int. Ed. Engl.* **33**, 317 (1994).
14. P. N. Rylander, *Catalytic Hydrogenation Over Platinum Metals* (Academic Press, New York, 1967), p. 424.
15. When C_6F_5D was used in reaction 7, only 1,4-C_6F_4HD was formed. Analysis of the recovered reactants revealed essentially no formation of C_6F_5H or of $(EtO)_3SiD$. Similarly, using $(EtO)_3SiD$ in reaction 7 resulted in exclusive formation of 1,4-C_6F_4HD. Analysis of recovered pentafluorobenzene revealed no exchange of H with D. This indicates a mechanism analogous to the one shown in Fig. 3 and excludes participation of a facile equilibrium

$$(EtO)_3SiRhL_3 + C_6F_5H \rightleftharpoons (EtO)_3SiH + C_6F_5RhL_3$$

16. Selected data for the reaction of **2**, $(EtO)_3SiH$, and C_6F_6 (1:120:450) are 94°C, 48 hours, and 38 turnovers for C_6F_5H; for the reaction of **2**, $(EtO)_3SiH$, and C_6F_5H (1:120:450), data are 94°C, 48 hours, and 33 turnovers for 1,4-$C_6F_4H_2$. The C_6F_6 and C_6F_5H used were rigorously checked for the presence of C_6F_5H and $C_6F_4H_2$, respectively, but none was found by ^1H and ^{19}F NMR. Control experiments (without **2** added) under the reaction conditions also did not yield these compounds.
17. W. E. Wentworth, T. Limero, E. C. M. Chen, *J. Phys. Chem.* **91**, 241 (1987).
18. B. E. Smart, in *The Chemistry of Functional Groups, Supplement D*, S. Patai and Z. Rappoport, Eds. (Wiley, New York, 1983), chap. 14.
19. Although the origin of regioselectivity is not clear, it is compatible with both electron transfer and nucleophilic oxidative addition. In both cases, the most polar C–F bond (the one para to H) is expected to be the most reactive.
20. C–F hydrogenolysis using heterogeneous catalysis was reported; reaction of polyfluorobenzenes is nonselective and requires very high temperatures [M. Hudlicky, *Chemistry of Organic Fluorine Compounds* (Prentice-Hall, New York, ed. 2, 1992), p. 175].
21. The drawing and data are given for one (of two) independent molecules of **3**.

22. We thank S. Cohen and F. Frolow for performing the x-ray crystallographic studies. Supported by the Basic Research Foundation, Jerusalem, Israel, and by the MINERVA Foundation, Munich, Germany. We are grateful to Hoechst, A-6, Frankfurt, Germany, for chemicals.

14 March 1994; accepted 1 June 1994

Probing Single Molecule Dynamics

X. Sunney Xie* and Robert C. Dunn

The room temperature dynamics of single sulforhodamine 101 molecules dispersed on a glass surface are investigated on two different time scales with near-field optics. On the 10^{-2}- to 10^{2}-second time scale, intensity fluctuations in the emission from single molecules are examined with polarization measurements, providing insight into their spectroscopic properties. On the nanosecond time scale, the fluorescence lifetimes of single molecules are measured, and their excited-state energy transfer to the aluminum coating of the near-field probe is characterized. A movie of the time-resolved emission demonstrates the feasibility of fluorescence lifetime imaging with single molecule sensitivity, picosecond temporal resolution, and a spatial resolving power beyond the diffraction limit.

Single molecule detection has recently been achieved at cryogenic temperatures (*1, 2*), in liquids with flow cytometry (*3*), in aerosol particles (*4*) and electrophoresis gels (*5*), and at interfaces with near-field optics (*6–9*). These results offer exciting possibilities in many fields, including analytical chemistry, materials research, and the biological sciences. In particular, near-field microscopy (*10*) permits the fluorescence imaging of single chromophores in ambient environments with nanometer spatial resolution (*6–9*). Moreover, Betzig and Chichester have recently shown that this technique can not only locate the single chromophores but also determine their orientations (*6*). Time-resolved spectroscopy combined with near-field optics (*11, 12*) will allow one to probe dynamical processes such as molecular motions and chemical reactions on a single molecule basis.

In near-field microscopy, sub–diffraction-limited spatial resolution is achieved by bringing a subwavelength spot of light close to a sample such that the resolution is only limited by the size of the spot. Single molecule sensitivity results from the high photon flux delivered by the tapered single mode fiber probe (*13*), efficient background rejection resulting from the small illumination area, and possibly, excitation by strong evanescent wave components near the tip end (*14*). The sides of the tapered near-field probe are coated with about 90 nm of aluminum to prevent light leakage, with an aperture of about 100 nm capable of delivering 10^{10} photons per second. A feedback mechanism based on shear force, similar to that previously reported (*15, 16*), is implemented to regulate the tip-sample gap with a vertical resolution of better than 1 nm. The total emission is collected from beneath a transparent sample by a detection

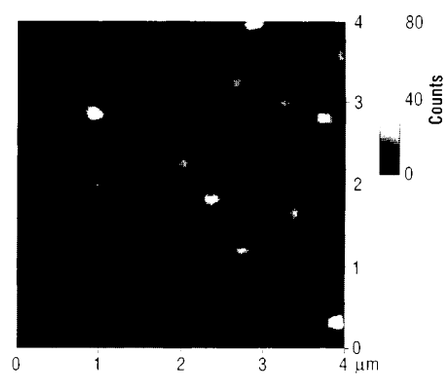

Fig. 1. Near-field fluorescence image of sulforhodamine 101 molecules dispersed on a glass surface. The bright features in the 4 μm by 4 μm (256 pixels by 256 pixels, 8-ms averaging time per pixel) image result from emission from single molecules. Linearly polarized excitation light aligned with the *x* axis was used. The FWHM of the sub–diffraction-limited features are 125 nm, which corresponds to the aperture diameter of the tip used in the imaging.

Pacific Northwest Laboratory, Molecular Science Research Center, P.O. Box 999, Richland, WA 99352, USA.

*To whom correspondence should be addressed.